Conformational Fluctuation Dynamics of Domain I of Human Serum Albumin in the Course of Chemically and Thermally Induced Unfolding Using Fluorescence Correlation Spectroscopy

ARTICLE *in* THE JOURNAL OF PHYSICAL CHEMISTRY B · APRIL 2014

Impact Factor: 3.3 · DOI: 10.1021/jp502762t · Source: PubMed

3 AUTHORS, INCLUDING:

Rajeev Yadav
Bowling Green State University
9 PUBLICATIONS **94** CITATIONS
SEE PROFILE

Bhaswati Sengupta
Indian Institute of Technology Kanpur
2 PUBLICATIONS **5** CITATIONS
SEE PROFILE

THE JOURNAL OF PHYSICAL CHEMISTRY B

Article

pubs.acs.org/JPCB

Conformational Fluctuation Dynamics of Domain I of Human Serum Albumin in the Course of Chemically and Thermally Induced Unfolding Using Fluorescence Correlation Spectroscopy

Rajeev Yadav, Bhaswati Sengupta, and Pratik Sen*

Department of Chemistry Indian Institute of Technology Kanpur, Kanpur 208 016, UP, India

Supporting Information

ABSTRACT: The present study elucidates the involvement of conformational fluctuation dynamics during chemically and thermally induced unfolding of human serum albumin (HSA) by fluorescence correlation spectroscopic (FCS) study, time-resolved fluorescence measurements, and circular dichroism (CD) spectroscopic methods. Two fluorescent probes, tetramethylrhodamine-5-maleimide (TMR) and *N*-(7-dimethylamino-4-methylcoumarin-3-yl) iodoacetamide (DACIA) were used to selectively label the domain I of HSA through the reaction with cys-34 for these studies. The guanidine hydrochloride (GnHCl) induced global structural change of HSA is monitored through its hydrodynamic radius (r_H) and CD response, which is found to be two step in nature. In FCS experiment, along with the diffusion time component we have observed an exponential relaxation time component (τ_R) that has been ascribed to the concerted chain dynamics of HSA. Unlike in the global structural change, we found that the τ_R value changes in a different manner in the course of the unfolding. The dependence of τ_R on the concentration of GnHCl was best fitted with a four state model, indicating the involvement of two intermediate states during the unfolding process, which were not observed through the CD response and r_H data. The fluorescence lifetime measurement also supports our observation of intermediate states during the unfolding of HSA. However, no such intermediate states were observed during thermally induced unfolding of HSA.

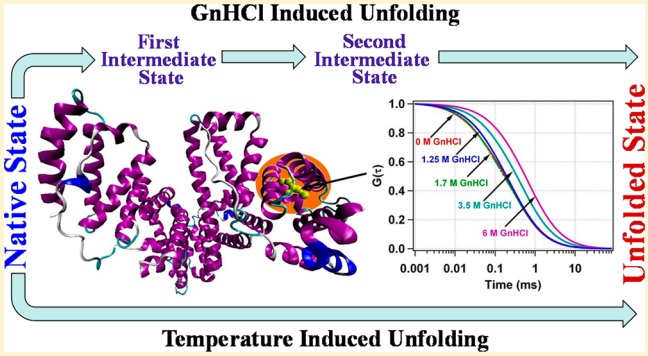

1. INTRODUCTION

Understanding the complex pathway of conformational changes during the folding/unfolding process of a protein is a major challenge in structural biology. A large numbers of experimental and theoretical studies have been performed to understand the unfolding pathway of proteins and are subject of considerable interest from the last few decades.[1−11] It not only requires the structural characterization during the unfolding process but also the elucidation of the structural dynamics is necessary. The structural dynamics of side chain is expected to be different for the compact (native) and the loosened (unfolded) state of the protein. The timescale of such chain dynamics is on the order of nanoseconds to microseconds and needs to be studied for a wide time window. In the present scenario, fluorescence-based methods like fluorescence anisotropy decay kinetics and fluorescence correlation spectroscopy (FCS) have become powerful tools to investigate the protein conformational dynamics in this time range.[5−34]

FCS is an elegant technique for studying the conformational dynamics of proteins,[5−14] DNA,[19−22] RNA,[23,24] polypeptides,[25] etc. in the submicrosecond to second timescale, which is based on the temporal fluctuation in the fluorescence intensity of a fluorescent probe attached to such macromolecules in the observation volume. The fluctuations of fluorescent intensity observed in FCS results either from the translational diffusion of the molecule or other processes that are faster than the diffusion time, e.g., intersystem crossing, cis−trans isomerization, fluorescence quenching, etc. The intensity fluctuation of a fluorescent tag attached to a protein can also arise from the quenching of the fluorescence signal of the fluorescent tag by some amino acid residues (act as quenchers), which is momentarily brought closer to the fluorescent tag by the conformational fluctuation of the side chain and can be studied by FCS.[26−28] Webb and co-workers have analyzed the conformational fluctuations of apomyoglobin as a function of acid-induced unfolding by FCS.[12] They have shown that as the pH of the medium decreases from 6.3 (native state) to 4.1 (molten globule state), both the fluctuation timescales and their amplitudes increase. Upon further decrease in the pH to 2.6 (unfolded state), the longer fluctuation time component as well as its amplitude remain constant; however, the amplitude of the shorter component increases from 11% to 17%.[12] They have reported the two time constants of conformational fluctuation of the native state as 8 and 100 μs. Samanta and co-workers

Received: March 20, 2014
Revised: April 22, 2014
Published: April 23, 2014

   dx.doi.org/10.1021/jp502762t | *J. Phys. Chem. B* 2014, 118, 5428−5438

Scheme 1. (a) Schematic representation of Human Serum Albumin (HSA) Showing Cys-34 Residue Where Fluorescent Probes, DACIA, and TMR have been Covalently Attached; Reaction of (b) *N*-(7-dimethylamino-4-methylcoumarin-3-yl) iodoacetamide (DACIA) and (c) tetramethylrhodamine-5-maleimide (TMR) with cys-34 of HSA

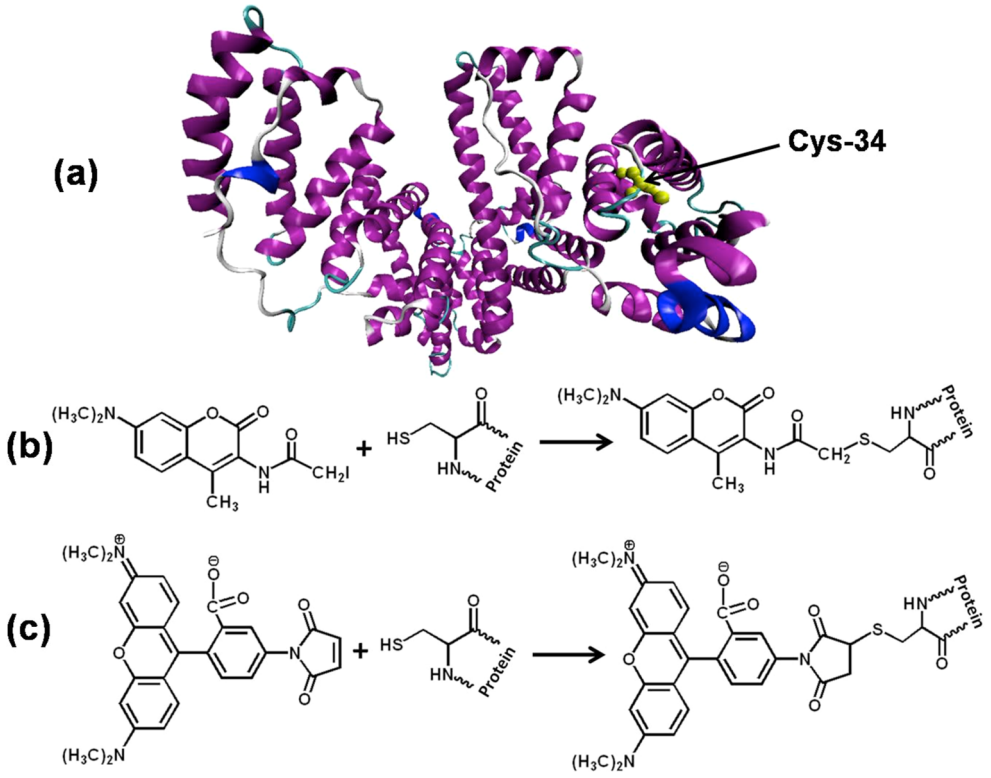

have studied the effect of dimethyl sulfoxide (DMSO) on the structure and the conformational dynamics of bovine serum albumin (BSA) labeled with FITC and observed that the hydrodynamic radius of BSA becomes almost double in the presence of 40% DMSO. The observed conformational dynamics of BSA with a time constant of 35 μs have been explained in terms of self-quenching of fluorescein isothiocyanate (FITC) fluorescence.[13] Frieden and co-workers have studied the kinetics of conformational fluctuation of a intestinal fatty acid binding protein and showed that the conformational fluctuations have a relaxation time component of 35 μs at pH 7.3 that becomes 2.5 μs at pH 2.[5,6]

Here we attempt to understand the structural fluctuations and conformational dynamics of domain I of HSA during thermally and chemically induced unfolding process through FCS. HSA is a large single chain multidomain protein with 585 amino acid residues and 17 disulfide bridges.[35,36] It is responsible for the transportation and deposition of wide varieties of metabolites and drugs in different parts of our body.[35,36] The structural characterization of HSA has been done by He et al. in 1992 followed by Curry et al. in 1998 crystallographically with a resolution of 2.8 and 2.5 Å, respectively.[37,38] Their study exhibits three structurally similar α-helical domains I, II, and III that forms a three-dimensional heart-shaped overall structure. Each domain is divided into two subdomains (denoted as A and B) and have a unique characteristic for binding different drugs and metabolites.[35−39] It is known that the properties of these domains are not identical and to understand the dynamics of the well-studied HSA, one has to gain knowledge of individual domains. In our previous study, we have shown that the domain III of HSA unfolds first followed by domains I and II on addition of GnHCl in the medium and also that the stabilization effect of sucrose on different domains of HSA are different.[40] Here, as a first choice, we chose domain I of HSA that contains only free cys-34 residue, which allows site-specific labeling by thiol-reactive fluorophores.[31,32,36] Many of the researchers have studied the dynamics of domain I through the change in the fluorescence properties of chromophores that are covalently attached with cys-34 of HSA.[1,10,11,31,32] Bright and co-workers have studied the dynamics of domain I of HSA through acrylodan attached covalently to cys-34.[32] Bhattacharyya and co-workers have studied the effect of room temperature ionic liquid (RTIL) on the size and conformational dynamics of domain I of HSA by FCS using the fluorescent probe, 7-dimethylamino-3-(4-maleimidophenyl)-4-methylcoumarin (CPM), covalently attached with cys-34. They have observed that RTIL acts as a denaturant when HSA is in its native state; however, it acts as a stabilizing agent in its unfolded state. Three time components have been ascribed to the conformational dynamics, among these, the two faster components were assigned for chain dynamics, while the slowest component has been assigned for interchain interaction or concerted motion.[9]

In the present work, we have explored the progressive variation in the conformational fluctuation dynamics of domain I of HSA during its chemically and thermally induced unfolding process using FCS. To provide additional information and to validate the conclusion, we have also used time-resolved fluorescence and circular dichroism (CD) spectroscopy. Two fluorescent probes, *N*-(7-dimethylamino-4-methylcoumarin-3-yl) iodoacetamide (DACIA) and tetramethylrhodamine-5-maleimide (TMR), were used to selectively label the domain I of HSA through the reaction with cys-34.

dx.doi.org/10.1021/jp502762t | J. Phys. Chem. B 2014, 118, 5428−5438

2. EXPERIMENTAL SECTION

2.1. Materials. Human serum albumin (HSA, essentially fatty acid free), tetramethylrhodamine-5-maleimide (TMR), and guanidine hydrochloride (GnHCl) were purchased from Sigma-Aldrich (St. Louis, MO) and used as received. *N*-(7-dimethylamino-4-methylcoumarin-3-yl) iodoacetamide (DACIA) has been purchased from Molecular Probes, Inc. and used as received. Analytical grade di-sodium hydrogen phosphate and sodium dihydrogen phosphate were purchased from Merck, India and used to prepare 50 mM buffer (pH 7.4). Dialysis membrane tubing (12 kDa cutoff) was purchased from Sigma-Aldrich and used after removing the glycerol and sulfur compounds, according to the procedure given by Sigma-Aldrich. Centrifugal filter units (Amicon Ultra, 10 kDa cutoff) have been purchased from Merck Millipore, Germany.

2.2. Protein Labeling and Sample Preparation. The labeling of HSA with DACIA and TMR were carried out following Wang et al.'s method with minor modification (Scheme 1).[1,41] Two stock solutions of ∼90 μM HSA were prepared in 50 mM phosphate buffer (pH 7.4) for each of the labeling dyes. Separately, the labeling dyes (DACIA and TMR) were dissolved in DMSO and added drop-by-drop to 6 mL of protein solution to a molar ratio of HSA to dye as 1:3.5. The mixture was then stirred gently at room temperature for 10 h followed by dialysis against 500 mL of 1:35 (v/v) DMSO and buffer (pH 7.4, 50 mM phosphate buffer) solution at 4 °C. The dialysis medium was replaced 4 times after each 12 h increment; afterward the dialysis medium was replaced by only buffer (pH 7.4, 50 mM phosphate buffer) for 6−8 days. To check whether dialysis was completed or not, we have recorded the fluorescence spectra of each dialyzed solution. The labeled protein was then concentrated using the 10 kDa cutoff centrifugal filtration unit. The concentration ratio of HSA and attached dye was estimated as ∼1:0.6 for both cases using absorbance of HSA, DACIA, and TMR and the molar extinction coefficient as 36500, 24000, and 75000 M^{-1} cm^{-1}, respectively.[41−43] The absorption and emission spectrum of free DACIA and TMR in buffer and labeled with cys-34 of HSA are shown in Figures S1 and S2 of the (Supporting Information). In all the experiments the samples were prepared in 50 mM phosphate buffer (pH 7.4), and the concentration of HSA was maintained as 10 and 2 μM for time-resolved fluorescence and circular dichroism (CD) measurements, respectively. However, for FCS measurements the concentration of HSA was maintained as 40 nM. All the measurements were done at 298 ± 1 K, if not stated otherwise.

2.3. Instrumentation and Methods. *Steady State Measurements.* The steady-state absorption and emission spectra were recorded in a commercial UV−visible spectrophotometer (Schimadzu 2450, Japan) and spectrofluorimeter (FluoroLog 3-21, Jobin Yvon, USA), respectively. Circular dichroism spectra were recorded in a commercial CD spectrometer (Jasco J-815, Japan).

Time-Resolved Fluorescence Measurements and Data Analysis. Time-resolved fluorescence intensity decays were collected using a commercial TCSPC setup (Life Spec II, Edinburgh Instruments, U.K.). All samples were excited at 376 nm and the full width at half-maxima of the instrument response function is 110 ps. For lifetime measurements, peak counts of 5000 were collected with the emission polarizer oriented at magic-angle polarization and decays were collected at 455 nm. The time-resolved fluorescence intensity decays were analyzed by deconvoluting the observed decays with the IRF to obtain the intensity decay function, manifested as a sum of three exponentials for the present study.[29]

$$I(t) = \sum_{i=1}^{3} fi \exp(-t/\tau_i) \tag{1}$$

where $I(t)$ is the fluorescence intensity at time t, f_i is the amplitude associated with the fluorescence lifetime τ_i, and the sum of all f values is unity.

FCS Measurements and Data Analysis. FCS measurements were performed on an instrument assembled in our laboratory, similar to that described in ref 44, consisting of an inverted confocal microscope Olympus IX-71. A 60× water immersion objective with NA 1.2 was used to focus the 532 nm excitation light, from a CW laser source (SDL-532-LN-002T, Sanghai Dream Laser Tech.), into the sample at a distance of 40 μm from the surface of the coverslip. The emitted photons were collected by the same objective and focused on a multimode fiber patch chord of 25 μm diameter (M67L01 25 μm 0.10NA, ThorLabs) after passing through a dichroic (ZT532rdc, Chroma Tech. Corp.) and an emission filter (605/70m, Chroma Tech. Corp.). A fluorescence signal was then directed toward a photon-counting module (SPCM-AQRH-13-FC, Excelitas Tech. Inc., Canada) through the fiber patch chord and then to the correlator card (Flex99OEM-12/E, Correlator.com) to generate the autocorrelation function $G(\tau)$. Finally, autocorrelation curves were displayed using LabView.

The autocorrelation function $G(\tau)$ of fluorescence fluctuations obtained from FCS experiment can be described as[29]

$$G(\tau) = \frac{\langle \delta F(t) \delta F(t+\tau) \rangle}{\langle F(t) \rangle^2} \tag{2}$$

where $\langle F(t) \rangle$ is the average fluorescence intensity, and $\delta F(t)$ and $\delta F(t+\tau)$ are the quantity of fluctuation in intensity around the mean value at time t and $t+\tau$ and are given by

$$\delta F(t) = F(t) - \langle F(t) \rangle,$$
$$\delta F(t+\tau) = F(t+\tau) - \langle F(t) \rangle \tag{3}$$

For a single-component system diffusing in only three dimensions in the solution phase, the diffusion time (τ_D) can be obtained by fitting the correlation function $G(\tau)$ using the following equation.[29]

$$G(\tau) = \frac{1}{N}\left(1 + \frac{t}{\tau_D}\right)^{-1}\left(1 + \frac{t}{\omega^2 \tau_D}\right)^{-1/2} \tag{4}$$

where N is the number of particles in the observation volume and $\omega = \omega_z/\omega_{xy}$, which is the depth-to-diameter ratio of 3D Gaussian volume. If the diffusing species undergoes an association chemical reaction or conformational change, which modulate its fluorescence intensity, with a relaxation time (τ_R) then the correlation function can be written as[12]

$$G(\tau) = \frac{1 - A + A \exp(-t/\tau_R)}{N(1-A)}\left(1 + \frac{t}{\tau_D}\right)^{-1}\left(1 + \frac{t}{\omega^2 \tau_D}\right)^{-1/2} \tag{5}$$

where A is the amplitude of the process defined by τ_R. The diffusion coefficient of the molecule can be calculated from the

dx.doi.org/10.1021/jp502762t | J. Phys. Chem. B 2014, 118, 5428−5438

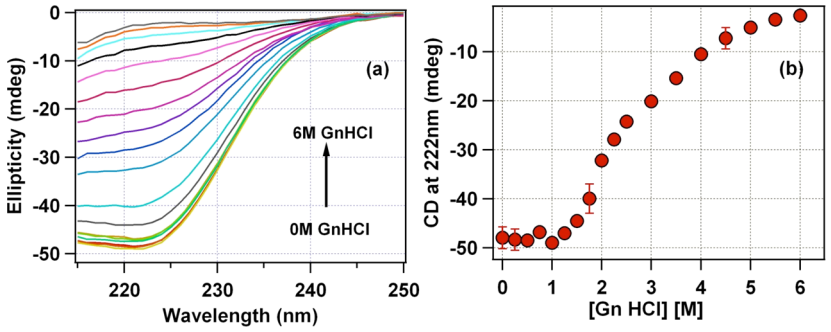

Figure 1. (a) Far-UV CD spectra of HSA in the absence and presence of different concentrations of GnHCl. (b) The change in the CD values at 222 nm with GnHCl concentration.

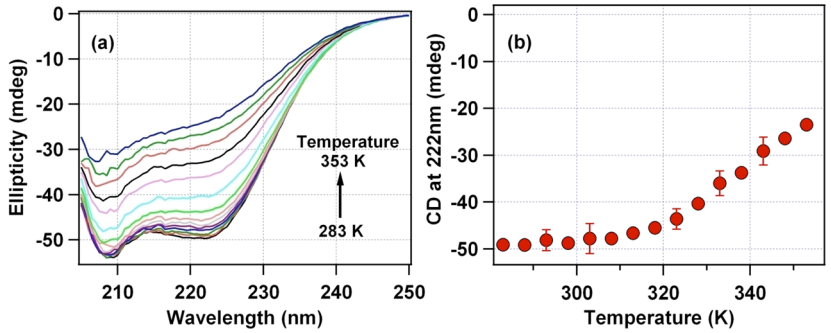

Figure 2. (a) Far-UV CD spectra of HSA at different temperatures. (b) The change in the CD values at 222 nm with temperature.

diffusion time (τ_D) and radius of the observation volume (ω_{xy}) using the following equation.

$$D_t = \frac{\omega_{xy}^2}{4\tau_D} \tag{6}$$

The structural parameter (ω) of the excitation volume was calibrated using a sample of known diffusion coefficient [Rhodamine 6G (R6G) in water, D_t = 4.14 × 10^{-6} cm^2 s^{-1}].[45] From the global analysis of the fluorescence correlation function of R6G of varying concentration, the observation volume has been estimated as 0.6 fL, with a transverse radius of 292 nm.

Finally, the hydrodynamic radius (r_H) of the molecule was determined from the diffusion coefficient (D_t) using the Stokes−Einstein equation as follows:[45]

$$r_H = \frac{k_B T}{6\pi\eta D_t} \tag{7}$$

where k_B is the Boltzmann constant, T is the absolute temperature (298 K in the present study), and η is the viscosity of the medium.

Here we used TMR-labeled HSA for the FCS study. TMR-labeled HSA was excited with 532 nm, and the fluctuation of its fluorescence was measured as a function of GnHCl in our home-built FCS system. Addition of GnHCl yields the changes in the viscosity and refractive index of the medium, which may affect the diffusion time in the observation volume. Refractive index mismatch can be corrected by adjusting the collar position of the objective as discussed in refs 44 and 46. In the present study, we have corrected the refractive index mismatch by adjusting the collar position of the objective from 0.14 in the absence of GnHCl to 0.20 in the presence of 6 M GnHCl. To determine the hydrodynamic radius of the protein accurately, viscosity correction has been done by measuring the diffusion time of R6G at each concentration of GnHCl as follows:[46,47]

$$\frac{r_H^{HSA}}{r_H^{R6G}} = \frac{\tau_D^{HSA}}{\tau_D^{R6G}} \tag{8}$$

Since R6G is rigid, its hydrodynamic radius (r_H^{R6G}) is independent of the viscosity of the medium, whereas the diffusion time of R6G molecule (r_D^{R6G}) will change with the change in the viscosity of the system. The r_H value of R6G has been calculated from the known value of D_t (4.14 × 10^{-6} cm^2 s^{-1}) using equation 6. The diffusion time of free R6G have also been determined in the presence of different concentrations of GnHCl for each experiment. The standardization with the R6G molecule mimics the exact experimental condition to minimize the effect of viscosity.

3. RESULTS

3.1. Circular Dichroism (CD) Spectroscopy. The CD spectrum of HSA exhibits two minima at 208 and 222 nm, signifying the α-helical signature of HSA.[48] Here, the change in the CD spectrum of HSA with increasing concentration of GnHCl is shown in Figure 1a. At a high concentration of GnHCl, we could not measure the CD spectra of HSA below 215 nm because of appreciable amounts of absorbance by GnHCl. Figure 1b shows the change in CD signal (mdeg) at 222 nm with increasing concentration of GnHCl. It shows that there is no change in α-helicity of HSA until 1.5 M GnHCl. This indicates that the protein retains its helical structure until 1.5 M GnHCl. On further increase in the GnHCl concentration, the CD signal at 222 nm starts changing rapidly and becomes almost constant at 5 M GnHCl. The result indicates that the secondary structure of HSA unfolds beyond 1.5 M GnHCl, and the unfolding process completed at 4.5 M GnHCl. This is in good agreement with previous reports, as

dx.doi.org/10.1021/jp502762t | J. Phys. Chem. B 2014, 118, 5428−5438

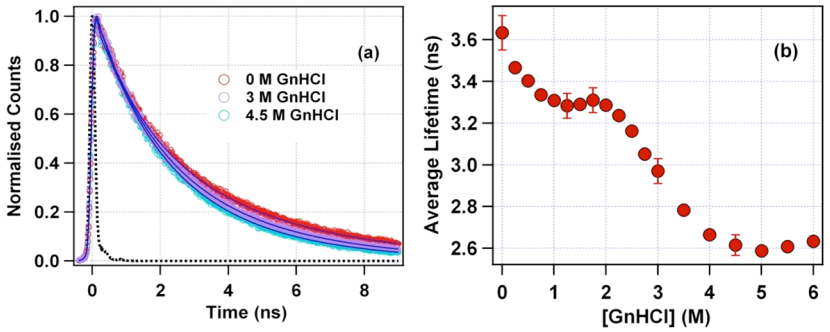

Figure 3. (a) Fluorescence transients of DACIA-HSA (λex = 376 nm and λem = 455 nm) at four different concentrations of GnHCl. Instrument response function is shown by a dashed line. Solid lines represent the best fit to a triexponential function. (b) The change in average lifetime of DACIA-HSA as a function of GnHCl concentration.

given by Ahmad et al. and Santra et al.[49,50] Figure 2 (panels a and b) shows the change in the CD spectrum of the HSA and CD signal (mdeg) at 222 nm with increase in temperature, respectively. It shows that the secondary structure of HSA remains unchanged until 310 K, and afterward, the helical structure starts destroying as the temperature rose. This is also in agreement with the previous report by Rezaei-Tavirani et al.[33]

3.2. Steady-State and Time-Resolved Fluorescence Spectroscopy. To study the effect of GnHCl and temperature solely on domain I of HSA, a fluorescent tag method was used. The nature of the signal of a fluorophore is a function of its local environment. Here we have attached a solvatochromic dye (DACIA) to cys-34 residue present in the domain I of HSA. The absorption maximum of DACIA in 50 mM phosphate buffer (pH 7.4) shows a peak at 379 nm and emission maximum at 478 nm. On labeling with HSA, the absorption maximum has been observed as 383 nm, and the emission maximum of DACIA changes dramatically with a large blue shift to 457 nm (Figure S1 of the Supporting Information). Upon unfolding (both chemically and thermally), the absorption spectrum of DACIA does not change much; however, the fluorescence response of DACIA is found to depend strongly on unfolding and shows an emission maximum of 478 and 461 nm in the presence of 6 M GnHCl (at 298 K and at 353 K, respectively). Along with the red shift in the emission maximum, the intensity of the fluorescence also decreased dramatically. For 6 M GnHCl, we have observed a 1.3 times decrease in the emission intensity from the native state, whereas upon increase of the temperature to 353 K, the emission intensity decreased by 1.7 times from 298 K.

To understand the system in a better way, the fluorescence transients of DACIA-labeled HSA were recorded in the presence of different concentrations of GnHCl varying from 0 to 6 M (at 298 K) and at different temperatures ranging from 283 to 353 K in the absence of GnHCl. The lifetime of DACIA-HSA have been evaluated by fitting these transients with three exponential decay models (equation 1). Figure 3a shows the fitted transients of DACIA labeled HSA using equation 1. The average lifetime of DACIA-HSA is found to depend strongly on the GnHCl concentration, as shown in Figure 3b and Table 1. This is to note that DACIA is covalently attached to domain I, and the change in the average lifetime of DACIA is obviously due the change in the local environment of domain I of HSA during the unfolding process. In the absence of GnHCl (at 298 K), the three time components of DACIA attached to HSA are 0.37 ns (0.03), 1.81 ns (0.22), and 4.28 ns (0.76) with an average lifetime 3.63 ns. As can be seen in Figure 3b, a shallow minimum is observed at 1.25 M GnHCl with an average lifetime of 3.28 ns. On further increase in GnHCl concentration to 1.75 M, the average lifetime increased to 3.32 ns. At 4.5 M GnHCl, the three time components are 0.13 ns (0.02), 1.65 ns (0.29), and 3.10 ns (0.69) with an average lifetime of 2.62 ns, which remains almost constant on further increase in the GnHCl concentration (Figure 3b, Table 1). Figure 4a shows the fluorescent transients of DACIA-labeled HSA at different temperatures (in absence of GnHCl), which is also observed to be triexponential in nature. At 283 K, the three time components of DACIA are 0.29 ns (0.01), 1.81 ns (0.20), and 4.32 ns (0.79) with an average lifetime of 3.78 ns. The average lifetime was found to decrease monotonically as the temperature was raised. At 353 K, the three components are 0.78 ns (0.09), 1.90 ns (0.32), and 3.72 ns (0.59) with an average lifetime of 2.87 ns. Figure 4b shows the change in the average lifetime of DACIA-labeled HSA in the course of the temperature-induced unfolding process. As mentioned earlier, the change in the average lifetime of DACIA in HSA is mainly because of the change in the local environment of domain I of HSA as DACIA is covalently attached to domain I.

Table 1. Average Fluorescence Lifetimes for DACIA Labeled HSA at Different GnHCl Concentration and Temperatures

	average lifetime		
GnHCl (M)	$\langle\tau\rangle$ (ns)	temperature (K)	$\langle\tau\rangle$ (ns)
0	3.63 ± 0.08	283	3.78
0.25	3.47	288	3.74
0.5	3.40	293	3.71
0.75	3.33	298	3.63 ± 0.08
1	3.31	303	3.61
1.25	3.28 ± 0.06	308	3.55
1.5	3.29	313	3.51
1.75	3.30 ± 0.06	318	3.49
2	3.29	323	3.45 ± 0.1
2.25	3.24	328	3.41
2.5	3.16	333	3.37 ± 0.07
2.75	3.05	338	3.30
3	2.97 ± 0.06	343	3.19 ± 0.07
3.5	2.78	348	3.03
4	2.67	353	2.87
4.5	2.62 ± 0.05		
5	2.59		
5.5	2.61		
6	2.63		

dx.doi.org/10.1021/jp502762t | J. Phys. Chem. B 2014, 118, 5428−5438

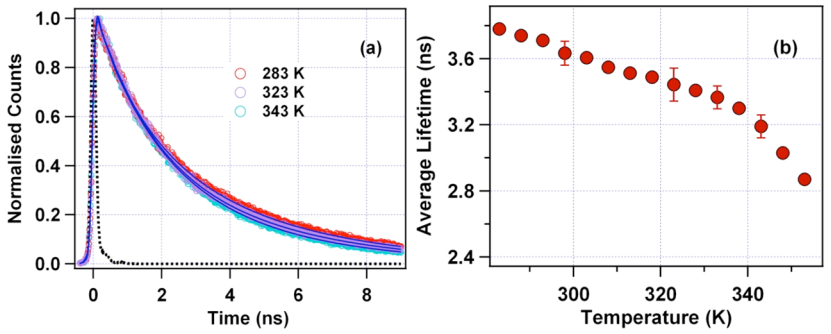

Figure 4. (a) Fluorescence transients of DACIA-HSA (λex = 376 nm and λem = 455 nm) at three different temperatures. Instrument response function is shown by a dashed line. Solid lines represent the best fit to a triexponential function. (b) The change in average lifetime of DACIA-HSA as a function of temperature.

Interestingly, the dependence of average lifetime of DACIA in HSA is not the same for chemically and thermally induced unfolding processes. In case of chemically induced unfolding, we have observed a shallow minimum, where as in the case of temperature induced unfolding, no such minimum was observed.

3.3. Fluorescence Correlation Spectroscopy. FCS study has been done with TMR-labeled HSA (attached to the same position where DACIA was tagged) in the absence and presence of different concentrations of GnHCl, varied from 0 to 6 M and at different temperatures varied from 283 to 343 K. The fluorescence autocorrelation traces were first attempted to fit using equation 4, which contains only one diffusion component, and we found that the fitting is inappropriate (see Figure S3, panels a and b, of the Supporting Information). Our next attempt was to include a distribution in diffusion time to fit the observed autocorrelation traces. Here we have used the Gaussian distribution model in our fitting equation as $G(\tau) = \sum a_i(\tau_{Di})(1 + \tau/\tau_{Di})^{-1}(1 + 1/\omega^2\tau_{Di})^{-1/2}$, where $a_i(\tau_{Di}) = A_i \exp(-\{[\ln(\tau_{Di}) - \ln(\tau_P)]/b\}^2)$, τ_P is the peak of the Gaussian distribution and b is the width of the distribution.[44,51] However, this model also fails to best-fit the autocorrelation traces (see Figure S4, panels a and b, of the Supporting Information), although the fitting is better than the fit using equation 4. The traces were best-fit to equation 5, which has one diffusion time component along with one exponential relaxation time component (see Figure 5 for some of the fitted autocorrelation curves and all are shown in Figure S5, panels a and b, of the Supporting Information). This implies that the source of the fluorescence intensity fluctuations is not only the diffusion of the TMR-HSA in and out of the observation volume but additionally guided by an exponential time component and has been assigned to the conformational changes of the protein within the observation volume.[12] A comparison of the fitting results with only one diffusion component, with a distribution in diffusion time, and one diffusion along with one exponential component, is shown in Figure S6 (panels a and b) of the Supporting Information for some GnHCl concentrations and for a few temperatures, respectively. The knowledge of the diffusion component will shed light on the hydrodynamic radius of the protein through the Stokes−Einstein relationship (eq 7), whereas the fluctuation relaxation time component gives the relaxation time for the conformational changes in the domain I of HSA. Bhattacharyya and co-workers as well as Samanta and co-workers also have observed such fluctuation relaxation time component for CPM-labeled HSA and FITC-labeled BSA, respectively.[9,13]

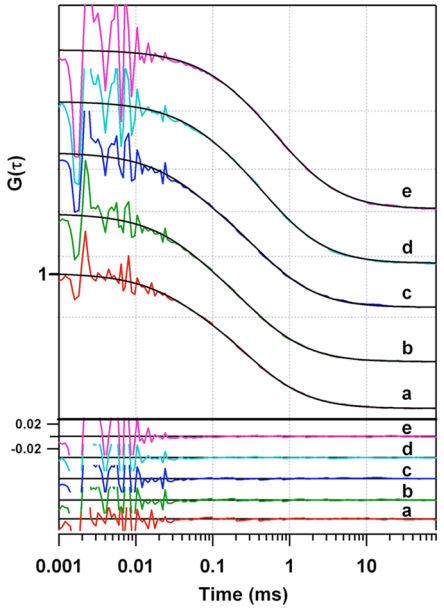

Figure 5. Autocorrelation curves of TMR-HSA in the presence of 0, 1.1, 2, 3.5, and 6 M GnHCl (a → e) with their best fit by equation 5 (1 diffusion + 1 exponential component model). Lower portion of this figure shows the fitting residuals of the respective curve.

Hydrodynamic Radius. The normalized fit lines of autocorrelation curves of TMR-HSA in the presence of six concentrations of GnHCl at 298 K are shown in Figure 6a and for five different temperatures in the absence of GnHCl are shown in Figure 6b. The correlation curve is found to shift toward the longer time region on increase in the concentration of GnHCl, indicating the slower diffusion (i.e., increase in the value of τ_D) of TMR-HSA upon unfolding. Both the increase in the size of HSA upon unfolding and the increase in viscosity of the medium by the presence of a high amount of GnHCl are responsible for the slow diffusion of TMR-HSA. However, these curves are found to shift toward a shorter time region upon increasing the temperature. This reverse behavior is because of the huge decrease in the viscosity of the sample with increase in the temperature that overcomes the effect of increase in the size of HSA upon thermal unfolding. The values of the experimentally measured τ_D have been employed to determine the diffusion coefficient (D_t) using equation 6, and the data are shown in Figure 7a for GnHCl-induced unfolding. In the absence of GnHCl, the measured value of τ_D is 252 ± 15 μs corresponding to D_t as 84.4 ± 5.4 $\mu m^2 s^{-1}$. On addition of

dx.doi.org/10.1021/jp502762t | J. Phys. Chem. B 2014, 118, 5428−5438

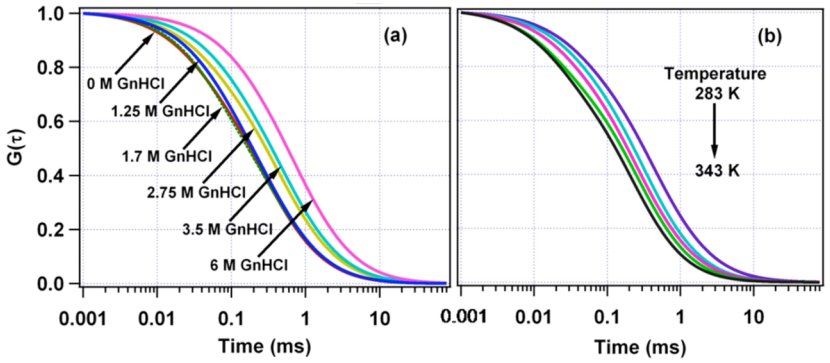

Figure 6. The normalized best fit lines of the autocorrelation curves of TMR-HSA by eq 5 (1 diffusion + 1 exponential component model) (a) in the presence of 0, 1.1, 1.7, 2.75, 3.5, 6 M GnHCl and (b) at different temperatures.

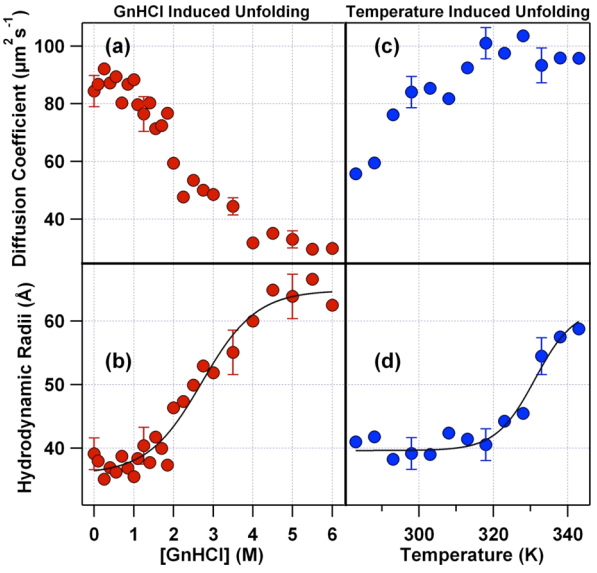

Figure 7. The change in diffusion coefficient, D_t, and hydrodynamic radii, r_H, of HSA as a function of GnHCl (a and b) concentration and (c and d) temperature. The solid line represents the data fitted into a two-state model.

GnHCl, the τ_D value gradually become slower and at 6 M GnHCl, the observed value is 712 μs with a D_t value of 29.9 $\mu m^2\ s^{-1}$. Since the viscosity of the solution is changing upon addition of GnHCl, the value of τ_D and D_t also incorporates the viscosity effect as already mentioned. The r_H value of HSA at each concentration of GnHCl has been determined after proper treatment of the τ_D value to correct the viscosity effect, as discussed in Instrumentation and Methods, and are tabulated in Table 2 and depicted in Figure 7b. In the native state of HSA, the r_H value is found to be 39.1 ± 2.5 Å, which is in good agreement with early reports as 38.4 ± 2.0 Å by Chowdhury et al.[28] using FCS, and 36 ± 1 Å by Galantini et al.[52] using small-angle X-ray scattering. Upon gradual addition of GnHCl to HSA, the value of r_H almost remains unchanged until 1.85 M; afterward, it increases continuously until 4.5 M GnHCl and observed as 64.9 Å. At further higher concentration of GnHCl, the value of r_H remains almost unchanged (see Figure 7b and Table 2), indicating that the overall structure of HSA is completely unfolded at 4.5 M GnHCl, which is in good agreement with our CD data. The value of r_H in the unfolded state of HSA is also in good agreement with the previous reports as 61.0 ± 3.0 Å by Sasmal et al.[9] According to Wilkins et al.[53] the r_H value for protein containing N number of amino acids in its native state as well as fully unfolded state can be obtained using the relations $r_H = (4.75 \pm 1.11)N^{0.29\pm0.02}$ Å and $r_H = (2.11 \pm 0.15)N^{0.57\pm0.02}$ Å, respectively. With the use of these relations, the r_H of HSA (N ∼ 585) has been calculated as 30.2 ± 10 Å and 79.7 ± 15 Å in its native and fully unfolded state, respectively. These numbers are also in good agreement with our observed values of r_H from FCS measurements.

Table 2. Diffusion Coefficient (D_t), Hydrodynamic Radius (r_H), and Concerted Chain Motion Time (τ_R) for TMR-Labeled HSA at Different GnHCl Concentrations

GnHCl (M)	D_t ($\mu m^2\ s^{-1}$)	r_H (Å)	τ_R (μs)
0	84.4 ± 5.4	39.1 ± 2.5	27.5 ± 5
0.1	86.8	38.0	30.9
0.25	92.1	35.1	29.3
0.4	87.2	36.9	28.3
0.55	89.4	36.2	29.4
0.7	80.3	38.7	29.2
0.85	86.8	36.8	32.9
1	88.3	35.5	31.3
1.1	79.7	38.4	39.8
1.25	76.5 ± 6	40.4 ± 2.9	52.4 ± 6
1.4	80.3	37.7	46.8
1.55	71.4	41.7	44.2
1.7	72.4	39.9	40.2
1.85	76.7	37.3	31.2
2	59.4	46.3	38.3
2.25	47.7	57.3	33.1
2.5	53.5	49.9	33.1
2.75	50.1	53.0	37.7
3	48.6	51.9	40.4
3.5	44.5 ± 3	55.1 ± 3.5	47.8 ± 6
4	31.8	73.1	60.5
4.5	35.1	64.9	74.4
5	33.6 ± 3	63.9 ± 3.5	72.9 ± 5
5.5	29.6	66.5	80.6
6	29.9	62.5	70.7

The values of diffusion coefficient (D_t) and hydrodynamic redii (r_H) have been determined for temperature-induced unfolding of TMR-HSA after incorporating the effect of change in viscosity as temperature raised and are tabulated in Table 3 and shown in Figure 7 (panels c and d), respectively. At 283 K, the value D_t and r_H has been observed as 57.7 $\mu m^2\ s^{-1}$ and 41.0 Å, respectively. At 298 K, the values of D_t and r_H are the same as we observed for 0 M GnHCl, as 84.4 ± 5.4 $\mu m^2\ s^{-1}$ and 39.1

dx.doi.org/10.1021/jp502762t | J. Phys. Chem. B 2014, 118, 5428−5438

Table 3. Diffusion Coefficient (D_t), Hydrodynamic Radius (r_H), and Concerted Chain Motion Time (τ_R) for TMR-Labeled HSA at Different Temperatures

temperature (K)	D_t (μm^2 s^{-1})	r_H (Å)	τ_R (μs)
283	55.7	40.9	27.0
288	59.5	41.8	28.8
293	76.2	38.2	27.2
298	84.4 ± 5.4	39.1 ± 2.5	27.5 ± 5
303	85.4	39.0	28.7
308	81.8	42.4	28.3
313	92.5	41.4	28.3
318	101.0 ± 5.4	40.5 ± 2.5	27.5 ± 5
323	97.5	44.2	29.1
328	103.5	45.5	25.1
333	93.3 ± 6	54.5 ± 2.9	28.7 ± 6
338	95.9	57.5	33.4
343	95.8	58.8	36.0

± 2.5 Å. On increase in the temperature to 343 K, the D_t and r_H become 99.2 μm^2 s^{-1} and 58.8 Å, respectively. It can be clearly seen that r_H values at different temperatures are in between the values in native and unfolded states of HSA, hence in good agreement with previous reports.

Conformational Dynamics. As stated earlier, the present FCS data are best-fit with a combination of diffusion (τ_D) and exponential time (τ_R) component as per equation 5. Like τ_D, the τ_R also comprises the viscosity effect,[6] hence, corrected for the viscosity following the method given by Mojumdar et al.[10] The corrected values of τ_R are shown in Figure 8 (panels a and b) for different GnHCl concentrations and temperatures, respectively, and are also tabulated in Tables 2 and 3, respectively. In the native state of HSA, at 298 K, τ_R is observed as 27.5 ± 5 μs and remain similar until 1 M GnHCl concentration. Afterward, an increment has been observed in the τ_R and reaches to 52.4 ± 6 μs at 1.25 M GnHCl. Upon further increase in the GnHCl concentration until 1.85 M, it decreased to 31.2 μs. The τ_R value again increases to 74.4 μs at 4.5 M GnHCl and remains similar until 6 M GnHCl. In the absence of GnHCl, at 283 K, τ_R is observed as 27.0 μs and is almost unchanged until 333 K; afterward it increases slowly and becomes 36.0 μs at 343 K.

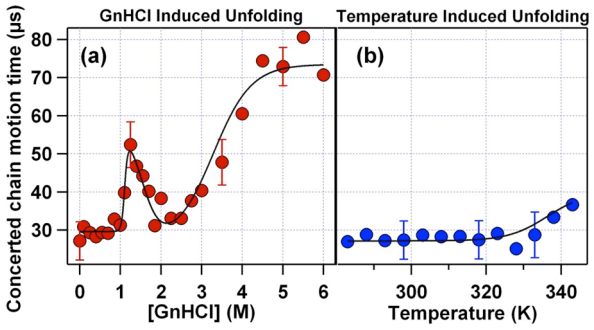

Figure 8. (a) Relaxation time component, τ_R corrected for viscosity and refractive index plotted as a function of GnHCl (a) concentration and (b) temperature. The solid line represents the data fitted into a four state model using equation 10.

The exponential time component observed from autocorrelation curves in the FCS experiment is in the timescale of 27–80 μs. Werner and co-workers have observed an ~30 μs time component of conformational dynamics of cytochrome c labeled with TMR in the intermediate state, which is in dynamic equilibrium with the unfolded state.[54] Webb and co-workers have observed an ~100 μs component in native and two components in the range of 30–200 μs, in the acid unfolded state of apomyoglobin and ascribed as concerted chain motions.[12] Samanta and co-workers have observed the similar relaxation time component of 35–80 μs and correlated to the conformational dynamics of BSA in the presence of DMSO.[13] Bhattacharyya and co-workers have observed three time components of conformational dynamics in the range of 3–200 μs for CPM-labeled HSA and attributed as the chain dynamics of the protein (faster components) and concerted chain motion (slower component).[9] In another work, they have shown that the time component of 35–55 μs is for a concerted chain motion of HSA in the absence and presence of different GnHCl concentrations.[10] Hence, in accordance with the above-mentioned reports, it can be concluded that the observed relaxation time constant of 27–80 μs is due to the concerted chain dynamics (concerted chain motion or interchain diffusion) of side chains of HSA, and τ_R has been assigned to concerted chain dynamics of domain I of HSA.

4. DISCUSSION

The primary goal of the present study is to understand the involvement of conformational fluctuation in domain I during the GnHCl and temperature-induced unfolding of HSA by FCS. The exponential time component observed in FCS experiment was assigned to the concerted chain motion dynamics in domain I of HSA, whereas the other time component was assigned to the diffusion of the whole protein. The diffusional time component is a measure of the overall size of the protein, and consequently, the hydrodynamic radius (r_H) was calculated. During the course of the unfolding process, the overall dependence of r_H on the GnHCl concentration and temperature matches with the result obtained from the CD spectroscopy. Both the studies indicate a two-state overall unfolding of HSA without the involvement of any stable intermediate state. However, as it can be seen in the fluorescence lifetime data, a shallow minimum was observed (see Figure 3b) at 1.25 M GnHCl with a local maxima at 1.75 M GnHCl. Such observation hints toward the involvement of intermediate state(s) in the unfolding pathway of HSA by GnHCl, whereas such signature of stable intermediate state(s) are absent in the temperature-induced unfolding process of HSA (see Figure 4b). This is to note that the fluorescence signal of the labeled fluorophore in HSA is mostly affected by its local environment. As here the fluorophore is tagged in domain I of HSA, we can assign the origin of the intermediate state because of subtle changes in domain I of HSA. However, such kind of intermediate state was not detected through CD and by measuring the r_H value through FCS.

The time component ascribed for concerted chain dynamics within the domain I of HSA originates from the fluctuation of fluorescence intensity of TMR through quenching by Tyr, His, and Phe amino acid residues present in the side chains.[55] On denaturation, the time constant of the concerted chain motion dynamics is expected to increase as the side chain of domain I of HSA would take longer time to come close to TMR because it has to diffuse through a long path in the unfolded state than in the native state.[12,13] The dependence of the time constant of the concerted chain dynamics (see Figure 8a) also indicate the involvement of intermediate state(s) during the GnHCl-induced unfolding, whereas such observation was not noted

dx.doi.org/10.1021/jp502762t | J. Phys. Chem. B 2014, 118, 5428–5438

Table 4. Fitting Parameters for GnHCl and Temperature-Induced Unfolding of TMR-Labeled HSA[a]

		N ↔ I_1			I_1 ↔ I_2			I_2 ↔ D		
		ΔG_1^0	m_1	$[D]_{1/2}$	ΔG_2^0	m_2	$[D]_{1/2}$	ΔG_3^0	m_3	$[D]_{1/2}$
	τ_R	16.76	15.02	1.12	4.34	2.79	1.56	4.17	1.27	3.28
GnHCl-induced unfolding		N ↔ D								
		ΔG^0	m	$[D]_{1/2}$						
	r_H	2.35	0.87	2.70						
temperature-induced unfolding		N ↔ D								
		ΔG^0	m	$[T]_{1/2}$						
	τ_R	38.0	0.11	345.5						
	r_H	37.4	0.11	340.0						

[a]Unit of ΔG^0 is kcal mol^{-1} and unit of m is kcal mol^{-1} M^{-1}. $[D]_{1/2}$ is the amount of GnHCl in M required for 50% unfolding and $[T]_{1/2}$ is the temperature in K required for 50% unfolding.

from the temperature-induced unfolding of HSA (see Figure 8b).

The dependence of concerted chain motion time during the GnHCl induced unfolding was best-fitted with four state model containing two intermediate states (see Figure 8a)

$$N \leftrightarrow I_1 \leftrightarrow I_2 \leftrightarrow U \tag{9}$$

where I_1 and I_2 are the two intermediate states in between the native (N) and unfolded (U) states of HSA. For such a four-state model, the overall spectroscopic signal(s) can be written as[17]

$$S = \frac{(S_N + S_{I1}\, e^{-X} + S_{I2}\, e^{-Y} + S_U\, e^{-Z})}{(1 + e^{-X} + e^{-Y} + e^{-Z})} \tag{10}$$

where,

$$X = (\Delta G_1^0 - m_1[GnHCl])/RT$$

$$Y = (\Delta G_1^0 + \Delta G_2^0 - (m_1 + m_2)[GnHCl])/RT$$

$$Z = (\Delta G_1^0 + \Delta G_2^0 + \Delta G_3^0 - (m_1 + m_2 + m_3)[GnHCl])/RT$$

and S_N, S_{I1}, S_{I2}, S_U are the values of the observable of the native, first intermediate, second intermediate, and unfolded state, respectively. ΔG_1^0, ΔG_2^0, and ΔG_3^0 are the free-energy change of each transition in the absence of denaturant. m_1, m_2 and m_3 are the slope of free-energy change plotted against the GnHCl. The concentration of denaturant to unfold 50% of the protein ($[D]_{1/2}$) can be calculated using the relation $[D]_{1/2} = \Delta G_i^0/m_i$. From the fitting parameters, the concerted chain motion time of N, I_1, I_2, and U states are found to be 29.6, 57, 27, and 73.4 μs, respectively. The observed values of ΔG^0, m, and $[D]_{1/2}$ for all three transitions are shown in Table 4. The $[D]_{1/2}$ value for the first transition (N ↔ I_1), second transition (I_1 ↔ I_2), and third transition (I_2 ↔ U) are estimated as 1.12, 1.56, and 3.28 M GnHCl, respectively. This clearly indicates the presence of two intermediate states during the unfolding process of HSA (Scheme 2) that exists in the initial concentration of GnHCl (until ~2 M GnHCl), which was not observed through CD and r_H values, where the variations could be best fit with a well-accepted two state model, N ↔ U.[40,50] The observed value of $[D]_{1/2}$ from the variation of r_H is found to be 2.7 M GnHCl concentration, which is in good agreement with the previously reported values.[40,50] For temperature-induced unfolding, the dependence of the concerted chain motion time was best fitted with the two state model N ↔ U, without the involvement of any intermediate state (see Figure 8b).

Scheme 2. Schematic Representation of GnHCl Induced Unfolding Process of HSA

$$N \longrightarrow I_1 \longrightarrow I_2 \longrightarrow U$$

5. CONCLUSIONS

In the present study, FCS has been employed to study the global structural change as well as conformational dynamics of HSA during chemically and thermally induced unfolding through the covalently attached fluorescent tag (TMR) in domain I. The global structure of HSA has been associated with an r_H value, which changes in a similar trend as observed through CD spectroscopy. The value of r_H has been observed as 39.1 ± 2.5 Å in the native state of HSA, and on addition of GnHCl it remains unchanged until 1.85 M, which become 64.9 Å in the presence of 4.5 M GnHCl. In fluorescence correlation spectroscopic study, an exponential relaxation time component (τ_R) has been observed along with the diffusion time component, and is ascribed to the concerted chain dynamics of domain I of HSA. The timescale of the concerted chain motion in the native state of HSA is found to be 27.5 ± 5 μs and remains similar until 1 M GnHCl. Afterward, an increment has been observed in the τ_R value which reaches to 52.4 ± 6 μs at 1.25 M GnHCl. Upon further increase in the GnHCl concentration until 1.85 M, the τ_R decreased to 31.2 μs. The τ_R value increases to 74.4 μs at 4.5 M GnHCl and remains similar to 6 M. Our analysis clearly indicates the involvement of two intermediate states during the GnHCl-induced unfolding process of HSA, and domain I of HSA is primarily responsible for this subtle change in the overall structure of the protein in the intermediate states, as the fluorescent probe is located in domain I of HSA. $[D]_{1/2}$ values for the first (N ↔ I_1), second (I_1 ↔ I_2), and third (I_2 ↔ D) transitions are estimated to be 1.16, 1.52, and 3.0 M, respectively. The fluorescence lifetime measurement also supports our observation of intermediate states during the GnHCl-induced unfolding of HSA. However, for thermally induced unfolding of HSA, no such intermediate states were observed. It has been realized that to completely understand the unfolding mechanism of such a massive protein, one needs to study the different fragment separately.

■ ASSOCIATED CONTENT

Supporting Information

The absorption and emission spectrum of free DACIA and TMR in buffer and labeled with cys-34 of HSA are shown in Figures S1 and S2. Autocorrelation curves of TMR-HSA in the

dx.doi.org/10.1021/jp502762t | J. Phys. Chem. B 2014, 118, 5428−5438

presence of different concentrations of GnHCl and at different temperatures with their best fit by equation 4 are shown in Figure S3 (panels a and b), respectively. Figure S4 (panels a and b) show the autocorrelation curves with the best fit by GDM analysis for different GnHCl concentrations and temperatures, respectively. Also, these autocorrelation curves with the best fit by equation 5 are shown in Figure S5 (panels a and b). A comparison in the fitting for equations 4 and 5 and GDM analysis is shown in Figure S6 (panels a and b) for some GnHCl concentrations and for a few temperatures, respectively. This material is available free of charge via the Internet at http://pubs.acs.org.

AUTHOR INFORMATION

Corresponding Author

*E-mail: psen@iitk.ac.in. Fax: +91-512-259-7436.

Notes

The authors declare no competing financial interest.

ACKNOWLEDGMENTS

R.Y. and B.S. thank the University Grant Commission and Council of Scientific & Industrial Research, Government of India, for awarding the fellowship. We also thanks Prof. S. Maiti (TIFR Mumbai, India) and Dr. S. Sen (JNU Delhi, India) for valuable suggestions to built the FCS setup. This work is financially supported by SERB, Government of India (Project no. SR/S1/PC-08/2011).

REFERENCES

(1) Amisha, J. K.; Zhao, L.; Zewail, A. H. Ultrafast Hydration Dynamics in Protein Unfolding: Human Serum Albumin. *Proc. Natl. Acad. Sci. U.S.A.* **2004**, *37*, 13411−13416.

(2) Klotz, I. M. Equilibrium Constants and Free Energies in Unfolding of Proteins in Urea Solutions. *Proc. Natl. Acad. Sci. U.S.A.* **1996**, *93*, 14411−14415.

(3) Ghosh, S.; Guchhait, N. Chemically Induced Unfolding of Bovine Serum Albumin by Urea and Sodium Dodecyl Sulfate: A Spectral Study with the Polarity-Sensitive Charge-Transfer Fluorescent Probe (E)-3-(4-Methylaminophenyl) acrylic Acid Methyl Ester. *ChemPhysChem* **2009**, *10*, 1664−1671.

(4) Anand, U.; Jash, C.; Mukherjee, S. Protein Unfolding and Subsequent Folding: A Spectroscopic Investigation. *Phys. Chem. Chem. Phys.* **2011**, *13*, 20418−20425.

(5) Chattopadhyay, K.; Saffarian, S.; Elson, E. L.; Frieden, C. Measurement of Microsecond Dynamic Motion in the Intestinal Fatty Acid Binding Protein by Using Fluorescence Correlation Spectroscopy. *Proc. Natl. Acad. Sci. U.S.A.* **2002**, *99*, 14171−14176.

(6) Chattopadhyay, K.; Elson, E. L.; Frieden, C. The Kinetics of Conformational Fluctuations in an Unfolded Protein Measured by Fluorescence Methods. *Proc. Natl. Acad. Sci. U.S.A.* **2005**, *102*, 2385−2389.

(7) Haldar, S.; Mitra, S.; Chattopadhyay, K. Role of Protein Stabilizers on the Conformation of the Unfolded State of Cytochrome c and Its Early Folding Kinetics: Investigation at Single Molecular Resolution. *J. Biol. Chem.* **2010**, *285*, 25314−25323.

(8) Haldar, S.; Chattopadhyay, K. Interconnection of Salt-Induced Hydrophobic Compaction and Secondary Structure Formation Depends on Solution Conditions. *J. Biol. Chem.* **2012**, *287*, 11546−11555.

(9) Sasmal, D. K.; Mondal, T.; Majumdar, S. S.; Choudhury, A.; Banerjee, R.; Bhattacharyya, K. An FCS Study of Unfolding and Refolding of CPM-Labeled Human Serum Albumin: Role of Ionic Liquid. *J. Phys. Chem. B* **2011**, *115*, 13075−13083.

(10) Mojumdar, S. S.; Chowdhury, R.; Chattoraj, S.; Bhattacharyya, K. Role of Ionic Liquid on the Conformational Dynamics in the Native, Molten Globule, and Unfolded State of Cytochrome C: A Fluorescence Correlation Spectroscopy Study. *J. Phys. Chem. B* **2012**, *116*, 12189−12198.

(11) Das, D. K.; Das, A. K.; Mandal, A. K.; Mondal, T.; Bhattacharyya, K. Effect of an Ionic Liquid on the Unfolding of Human Serum Albumin: A Fluorescence Correlation Spectroscopy Study. *ChemPhysChem* **2012**, *13*, 1949−1955.

(12) Chen, H.; Rhoades, E.; Butler, J. S.; Loh, S. N.; Webb, W. W. Dynamics of Equilibrium Structural Fluctuations of Apomyoglobin Measured by Fluorescence Correlation Spectroscopy. *Proc. Natl. Acad. Sci. U.S.A.* **2007**, *104*, 10459−10464.

(13) Pabbathi, A.; Patra, S.; Samanta, A. Structural Transformation of Bovine Serum Albumin Induced by Dimethyl Sulfoxide and Probed by Fluorescence Correlation Spectroscopy and Additional Methods. *ChemPhysChem* **2013**, *14*, 2441−2449.

(14) Patra, S.; Santhosh, K.; Pabbathi, A.; Samanta, A. Diffusion of Organic Dyes in Bovine Serum Albumin Solution Studied by Fluorescence Correlation Spectroscopy. *RSC Adv.* **2012**, *2*, 6079−6086.

(15) Rami, B. R.; Krishnamoorthy, G.; Udgaonkar, J. B. Dynamics of the Core Tryptophan During the Formation of a Productive Molten Globule Intermediate of Barstar. *Biochemistry* **2003**, *42*, 7986−8000.

(16) Jha, A.; Ishii, K.; Udgaonkar, J. B.; Tahara, T.; Krishnamoorthy, G. Exploration of the Correlation Between Solvation Dynamics and Internal Dynamics of a Protein. *Biochemistry* **2011**, *50*, 397−408.

(17) Naidu, K. T.; Prabhu, N. P. Protein Surfactant Interaction: Sodium Dodecyl Sulfate-Induced Unfolding of Ribonuclease A. *J. Phys. Chem. B* **2011**, *115*, 14760−14767.

(18) Fuentealba, D.; Kato, H.; Nishijima, M.; Fukuhara, G.; Mori, T.; Inoue, Y.; Bohne, C. Explaining the Highly Enantiomeric Photocyclodimerization of 2-Anthracenecarboxylate Bound to Human Serum Albumin Using Time-Resolved Anisotropy Studies. *J. Am. Chem. Soc.* **2013**, *135*, 203−209.

(19) Li, H. T.; Ren, X. J.; Ying, L. M.; Balasubramanium, S.; Klenerman, D. Measuring Single-Molecule Nucleic Acid Dynamics in Solution by Two-Color Filtered Ratiometric Fluorescence Correlation Spectroscopy. *Proc. Natl. Acad. Sci. U.S.A.* **2004**, *101*, 14425−14430.

(20) Jung, J.; Orden, A. V. A Three-State Mechanism for DNA Hairpin Folding Characterized by Multiparameter Fluorescence Fluctuation Spectroscopy. *J. Am. Chem. Soc.* **2006**, *128*, 1240−1249.

(21) Edman, L.; Mets, U.; Rigler, R. Conformational Transitions Monitored for Single Molecules in Solution. *Proc. Natl. Acad. Sci. U.S.A.* **1996**, *93*, 6710−6715.

(22) Ishii, K.; Tahara, T. Two-Dimensional Fluorescence Lifetime Correlation Spectroscopy. 2. Application. *J. Phys. Chem. B* **2013**, *117*, 11423−11432.

(23) Kim, H. D.; Nienhaus, G. U.; Ha, T.; Orr, J. W.; Williamson, J. R.; Chu, S. Mg^{2+}-Dependent Conformational Change of RNA Studied by Fluorescence Correlation and FRET on Immobilized Single Molecules. *Proc. Natl. Acad. Sci. U.S.A.* **2002**, *99*, 4284−4289.

(24) Kim, J.; Doose, S.; Neuweiler, H.; Sauer, M. The Initial Step of DNA Hairpin Folding: A Kinetic Analysis Using Fluorescence Correlation Spectroscopy. *Nucleic Acids Res.* **2006**, *34*, 2516−2527.

(25) Neuweiler, H.; Doose, S.; Sauer, M. A Microscopic View of Miniprotein Folding: Enhanced Folding Efficiency Through Formation of an Intermediate. *Proc. Natl. Acad. Sci. U.S.A.* **2005**, *102*, 16650−16655.

(26) Neuweiler, H.; Banachewicz, W.; Fersht, A. R. Kinetics of Chain Motions Within a Protein-Folding Intermediate. *Proc. Natl. Acad. Sci. U.S.A.* **2010**, *107*, 22106−22110.

(27) Neuweiler, H.; Johnson, C. M.; Fersht, A. R. Direct Observation of Ultrafast Folding and Denatured State Dynamics in Single Protein Molecules. *Proc. Natl. Acad. Sci. U.S.A.* **2009**, *106*, 18569−18574.

(28) Chowdhury, R.; Chattoraj, S.; Mojumdar, S. S.; Bhattacharyya, K. FRET Between a Donor and an Acceptor Covalently Bound to Human Serum Albumin in Native and Non-Native States. *Phys. Chem. Chem. Phys.* **2013**, *15*, 16286−16293.

(29) Lakowicz, J. R. *Principles of Fluorescence Spectroscopy*, 3rd Ed.; Springer: NY, 2006.

(30) Jha, A.; Udgaonkar, J. B.; Krishnamoorthy, G. Characterization of the Heterogeneity and Specificity of Inter-Polypeptide Interactions in Amyloid Protofibrils by Measurement of Site-Specific Fluorescence Anisotropy Decay Kinetics. *J. Mol. Biol.* **2009**, *393*, 735−752.
(31) Flora, K.; Brennan, J. D.; Baker, G. A.; Doody, M. A.; Bright, F. V. Unfolding of Acrylodan-Labeled Human Serum Albumin Probed by Steady-State and Time-Resolved Fluorescence Methods. *Biophys. J.* **1998**, *75*, 1084−1096.
(32) Page, T. A.; Kraut, N. D.; Page, P. M.; Baker, G. A.; Bright, F. V. Dynamics of Loop 1 of Domain I in Human Serum Albumin When Dissolved in Ionic Liquids. *J. Phys. Chem. B* **2009**, *113*, 12825−12830.
(33) Rezaei-Tavirani, M.; Moghaddaminia, S. H.; Ranjbar, B.; Amani, M.; Marashi, S. A. Conformational Study of Human Serum Albumin in Pre-Denaturation Temperature by Differential Scanning Calorimetry, Circular Dichroism and UV Spectroscopy. *J. Biochem. Mol. Biol.* **2006**, *39*, 530−536.
(34) Sahu, K.; Mondal, S. K.; Ghosh, S.; Roy, D.; Bhattacharyya, K. Temperature Dependence of Solvation Dynamics and Anisotropy Decay in a Protein: ANS in Bovine Serum Albumin. *J. Chem. Phys.* **2006**, *124*, 124909.
(35) Dugiaczyk, A.; Law, S.; Dennison, O. E. Nucleotide Sequence and the Encoded Amino Acids of Human Serum Albumin mRNA. *Proc. Natl. Acad. Sci. U.S.A.* **1982**, *79*, 71−75.
(36) Peters, T., Jr. *All About Albumin: Biochemistry, Genetics, and Medical Applications*; Academic Press: San Diego, 1996.
(37) He, X. M.; Carter, D. C. Atomic Structure and Chemistry of Human Serum Albumin. *Nature* **1992**, *358*, 209−215.
(38) Curry, S.; Mandelkow, H.; Brick, P.; Franks, N. Crystal Structure of Human Serum Albumin Complexed with Fatty Acid Reveals an aAsymmetric Distribution of Binding Sites. *Nat. Struct. Biol.* **1998**, *5*, 827−835.
(39) Sugio, S.; Kashima, A.; Mochizuki, S.; Noda, M.; Kobayashi, K. Crystal Structure of Human Serum Albumin at 2.5 Å Resolution. *Protein Eng.* **1999**, *12*, 439−446.
(40) Yadav, R.; Sen, P. Mechanistic Investigation of Domain Specific Unfolding of Human Serum Albumin and the Effect of Sucrose. *Protein Sci.* **2013**, *22*, 1571−1581.
(41) Wang, R.; Sun, S.; Bekos, E.; Bright, F. V. Dynamics Surrounding Chemically Denatured, Serum Albumin Cys-34 in Native, and Silicam-Adsorbed Bovine Serum Albumin. *Anal. Chem.* **1995**, *67*, 149−159.
(42) 2.3 Thiol-reactive probes excited with ultraviolet light, Invitrogen.
(43) Kwon, G.; Remmers, A. E.; Datta, S.; Neubig, R. R. Synthesis and Characterization of Fluorescently Labeled Bovine Brain G Protein Subunits. *Biochemistry* **1993**, *32*, 2401−2408.
(44) Pal, N.; Verma, S. D.; Singh, M. K.; Sen, S. Fluorescence Correlation Spectroscopy: An Efficient Tool for Measuring Size, Size-Distribution and Polydispersity of Microemulsion Droplets in Solution. *Anal. Chem.* **2011**, *83*, 7736−7744.
(45) Müller, C. B.; Loman, A.; Pacheco, V.; Koberling, F.; Willbold, D.; Richtering, W.; Enderlein, J. Precise Measurement of Diffusion by Multi-Color Dual-Focus Fluorescence Correlation Spectroscopy. *Europhys. Lett.* **2008**, *83*, 46001.
(46) Chattopadhyay, K.; Saffarian, S.; Elson, E. L.; Frieden, C. Measuring Unfolding of Protein in the Presence of Denaturant Using Fluorescence Correlation Spectroscopy. *Biophys. J.* **2005**, *88*, 1413−1422.
(47) Sherman, E.; Itkin, A.; Kuttner, Y. Y.; Rhoades, E.; Amir, D.; Haas, E.; Haran, G. Using Fluorescence Correlation Spectroscopy to Study Conformational Changes in Denatured Proteins. *Biophys. J.* **2008**, *94*, 4819−4827.
(48) Kelly, S. M.; Price, N. C. The Use of Circular Dichroism in the Investigation of Protein Structure and Function. *Curr. Protein Pept. Sci.* **2000**, *1*, 349−384.
(49) Ahmad, B.; Ahmad, M. Z.; Haq, S. K.; Khan, R. H. Guanidine Hydrochloride Denaturation of Human Serum Albumin Originates by Local Unfolding of Some Stable Loops in Domain III. *Biochim. Biophys. Acta* **2005**, *1750*, 93−102.
(50) Santra, M. K.; Banerjee, A.; Krishnakumar, S. S.; Rahaman, O.; Panda, D. Multiple-Probe Analysis of Folding and Unfolding Pathways of Human Serum Albumin. *Eur. J. Biochem.* **2004**, *271*, 1789−1797.
(51) Sharma, S.; Pal, N.; Chowdhury, P. K.; Sen, S.; Ganguli, A. K. Understanding Growth Kinetics of Nanorods in Microemulsion: A Combined Fluorescence Correlation Spectroscopy, Dynamic Light Scattering, and Electron Microscopy Study. *J. Am. Chem. Soc.* **2012**, *134*, 19677−19684.
(52) Galantini, L.; Leggio, C.; Konarev, P. V.; Pavel, N. V. Human Serum Albumin Binding Ibuprofen: A 3D Description of the Unfolding Pathway in Urea. *Biophys. Chem.* **2010**, *147*, 111−122.
(53) Wilkins, D. K.; Grimshaw, S. B.; Receveur, V.; Dobson, C. M.; Jones, J. A.; Smith, L. J. Hydrodynamic Radii of Native and Denatured Proteins Measured by Pulse Field Gradient NMR Techniques. *Biochemistry* **1999**, *38*, 16424−16431.
(54) Werner, J. H.; Joggerst, R.; Dyer, R. B.; Goodwin, P. M. A Two-Dimensional View of the Folding Energy Landscape of Cytochrome c. *Proc. Natl. Acad. Sci. U.S.A.* **2006**, *103*, 11130−11135.
(55) Hirano, M.; Takeuchi, Y.; Aoki, T.; Yanagida, T.; Ide, T. Rearrangements in the KcsA Cytoplasmic Domain Underlie its Gating. *J. Biol. Chem.* **2010**, *285*, 3777−3783.